Journal of Organometallic Chemistry, 372 (1989) 129–139
Elsevier Sequoia S.A., Lausanne – Printed in The Netherlands
JOM 09868

Mixed metal clusters: structural and reactivity trends

Tapani A. Pakkanen, Jouni Pursiainen, Tapani Venäläinen and Tuula T. Pakkanen
Department of Chemistry, University of Joensuu, P.O. Box 111, SF-80101 Joensuu (Finland)

(Received November 28th, 1988)

Abstract

The results from a systematic synthesis and trends in structural and physical properties and chemical reactivity for a large group of clusters are valuable for the understanding of the role of a particular element in a mixed metal cluster. As an example tetrahedral $H_xM_4(CO)_{12}$ clusters, where M represents metals Fe, Ru, Co and Rh or their combinations, are discussed in detail. Their metal–metal bond distances and ^1H NMR parameters are presented as a function of metal composition. Similar trends are also shown for their reactivity towards phosphine substitution.

1. Introduction

Mixed metal clusters with metal–metal bonding are found around the periodic table of elements. Halide clusters of the early transition elements form mixed metal systems, but very few systematic studies, where the metal composition covers a wide range are available. Phosphorus and sulfur ligand stabilized clusters of gold and a few neighboring elements are in the same state with respect to the systematic knowledge of mixed metal systems. Zintl ion clusters form also mixed metal systems some of which span a useful range for systematic comparisons [1]. On the right of the periodic table clusters open up to cages, rings and chains, where mixed element systems are also possible [2].

The best known area of mixed metal clusters are mixed metal carbonyl clusters. There is a large group of such compounds with many metal combinations, where numerous studies from the last three decades are available. Metal carbonyls are also the most widely used clusters in applications.

For a detailed systematic survey of mixed metal trends, it is practical to limit the discussion to clusters of specific nuclearity and framework. Di- and tri-metallic carbonyl systems offer only limited structural possibilities and the low nuclearity does not allow several different elements in the same molecule. Tetranuclear clusters have less structural limitations, and a large number of studies are available. Clusters

0022-328X/89/$03.50

of higher nuclearity are even more versatile for systematic variation of the metal composition, but only a few such studies are available. However, with high nuclearity, the number of metal combinations and structural isomers becomes rapidly very large, leading to complex mixtures. The discussion of the trends will focus on tetranuclear mixed metal carbonyl clusters.

2. Closed tetranuclear mixed metal carbonyls

Even for tetranuclear clusters there is a large variety of different possible cluster geometries. The most homogeneous group within the tetranuclear clusters is formed by the closed tetrahedral systems. Another large group of mixed metal tetranuclear clusters are the open butterfly clusters [3]. The closed clusters can be conveniently classified by the number of different elements in the cluster. A review of literature shows that most studies have been published for iron and cobalt group metals, where iron, ruthenium, cobalt and rhodium clusters are best represented [4]. Fig. 1 shows all possible tetranuclear Fe–Ru–Co–Rh combinations. If examples of all these clusters were known and characterized, a comprehensive understanding of the influence of the metal composition on the cluster properties could be obtained. Structural information is not available for most of the iron containing clusters, only the Fe–Ru clusters are reasonably well represented. The best structurally char-

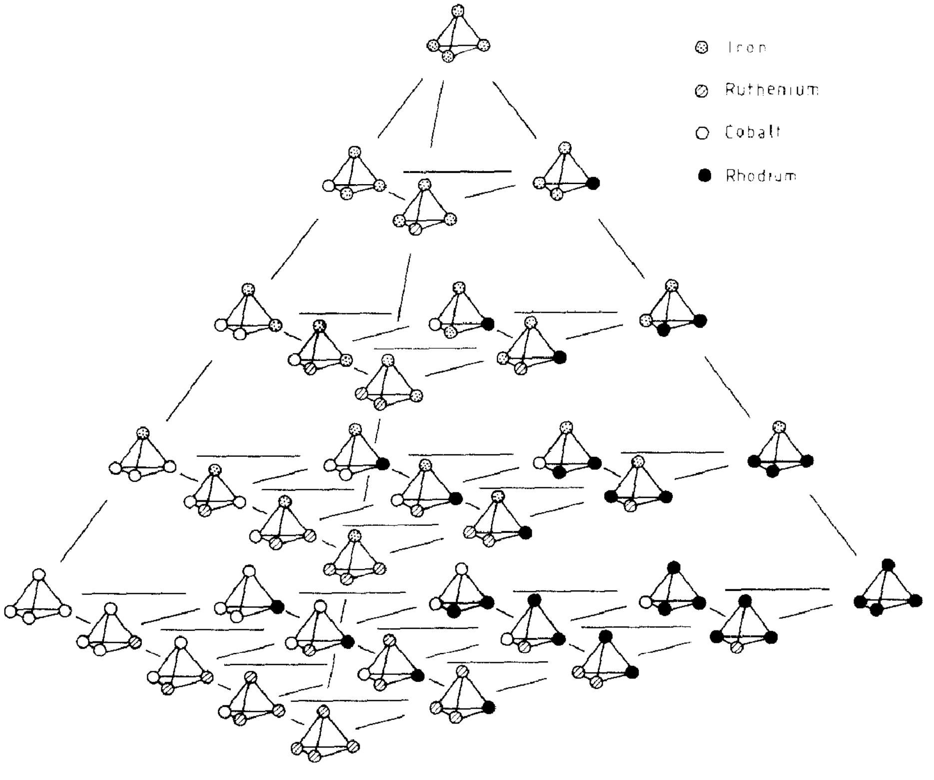

Fig. 1. All possible mixed metal combinations for tetranuclear clusters of iron, ruthenium, cobalt and rhodium.

acterized coherent group is formed by the $H_xM_4(CO)_{12}$ mixed metal clusters of ruthenium, cobalt and rhodium.

3. $H_xM_4(CO)_{12}$ clusters of ruthenium, cobalt and rhodium

Of the fifteen possible parent $H_xM_4(CO)_{12}$ (M = Ru, Co or Rh) mixed metal clusters $CoRh_3(CO)_{12}$ is unstable [4] (Fig. 2). While the Ru_3Rh core is represented by $H_2Ru_3Rh(CO)_{10}(C_5H_5)$ [5], for all the others parent mixed metal carbonyls (or hydrides) are known. X-ray structures are available for $H_4Ru_4(CO)_{12}$ [6], $H_3Ru_3Co(CO)_{12}$ [7], $H_2Ru_2Co_2(CO)_{12}$ [8], $H_2Ru_2Rh_2(CO)_{12}$ [9], $HRuRh_3(CO)_{12}$ [10], $Co_4(CO)_{12}$ [11,12] and $Rh_4(CO)_{12}$ [11]. $H_2Ru_2CoRh(CO)_{12}$ [13], $HRuCo_2Rh(CO)_{12}$ [13], $HRuCoRh_2(CO)_{12}$ [13], $HRuCo_3(CO)_{12}$ [14], $Co_3Rh(CO)_{12}$ [4,15] and $Co_2Rh_2(CO)_{12}$ [4] have been characterized spectroscopically.

3.1. Site selective reactions

Phosphine derivatives have been prepared for most of the $H_xM_4(CO)_{12}$ mixed metal clusters of Fig. 2. There are several examples of phosphines coordinating to rhodium in Co–Rh [16] and Ru–Rh [10,17] mixed metal clusters. Preference between ruthenium and cobalt is not clear since both Ru and Co coordinated phosphines have been found in the Ru–Co clusters [18]. These preferences correspond well with the recent observations in trinuclear $(\mu_3\text{-X})RuCo_2(CO)_9$ (X = alkyne, vinylidene, sulfur, phosphinidene) mixed-metal clusters [19].

Most of the homometallic and heterometallic clusters up to two elements have been synthesized via special routes in which the separation problems can be avoided. Site selective reactions can be useful for the separation of complex cluster mixtures. In Fig. 3 an example is shown of the use of site selective coordination as a means of separation. The starting point is the reaction of rhodate anion $[Rh(CO)_4]^-$ with $RuCo_2(CO)_{11}$:

$$[Rh(CO)_4]^- + RuCo_2(CO)_{11} \xrightarrow[(2)\ H_3PO_4]{(1).\ THF,\ 1\ h}$$

$$\underset{(x = 0\text{–}3)}{HRuCo_xRh_{3-x}(CO)_{12}} + \underset{(x = 0,\ 1)}{H_2Ru_2Co_xRh_{2-x}(CO)_{12}}$$

The products were characterized by ^1H NMR spectroscopy (Fig. 4) [13]. Selective decoupling experiments and comparisons with spectra of the known components of the mixture allow an unambiguous assignment. The main components of the reaction mixture are $HRuCo_xRh_{3-x}(CO)_{12}$ ($x = 0$–3) as shown in the first row of Fig. 3. Ligand substitution reactivity trends can be used to separate mixed metal cores in the following reaction sequence. At low temperature a monosubstitution takes place only on rhodium; thus $HRuCo_3(CO)_{12}$ can be separated. At room temperature a disubstitution occurs at rhodium, allowing the separation of $HRuCo_2Rh(CO)_{11}PPh_3$. Similarly $HRuCoRh_2(CO)_{10}(PPh_3)_2$ can be separated at higher temperatures.

3.2. Geometric trends

Discussion of detailed geometrical trends requires a complete set of mixed metal structures, which is not available even for tetranuclear Ru–Co–Rh clusters. The

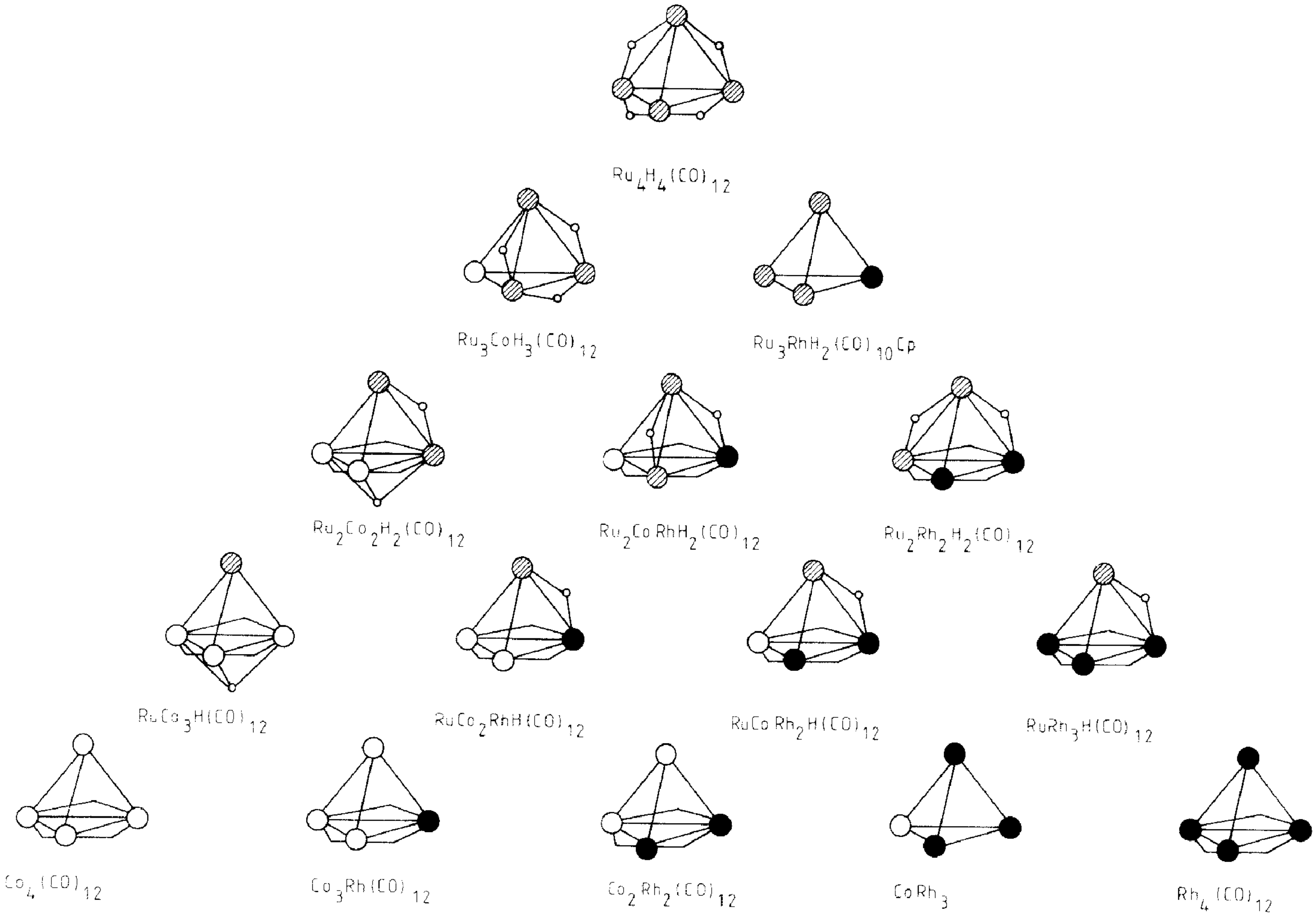

Fig. 2. Tetranuclear mixed metal clusters $H_xRu_xCo_yRh_z(CO)_{12}$, where $x + y + z = 4$. **Hydrogens** are shown with small open circles, bridging carbonyls with solid lines.

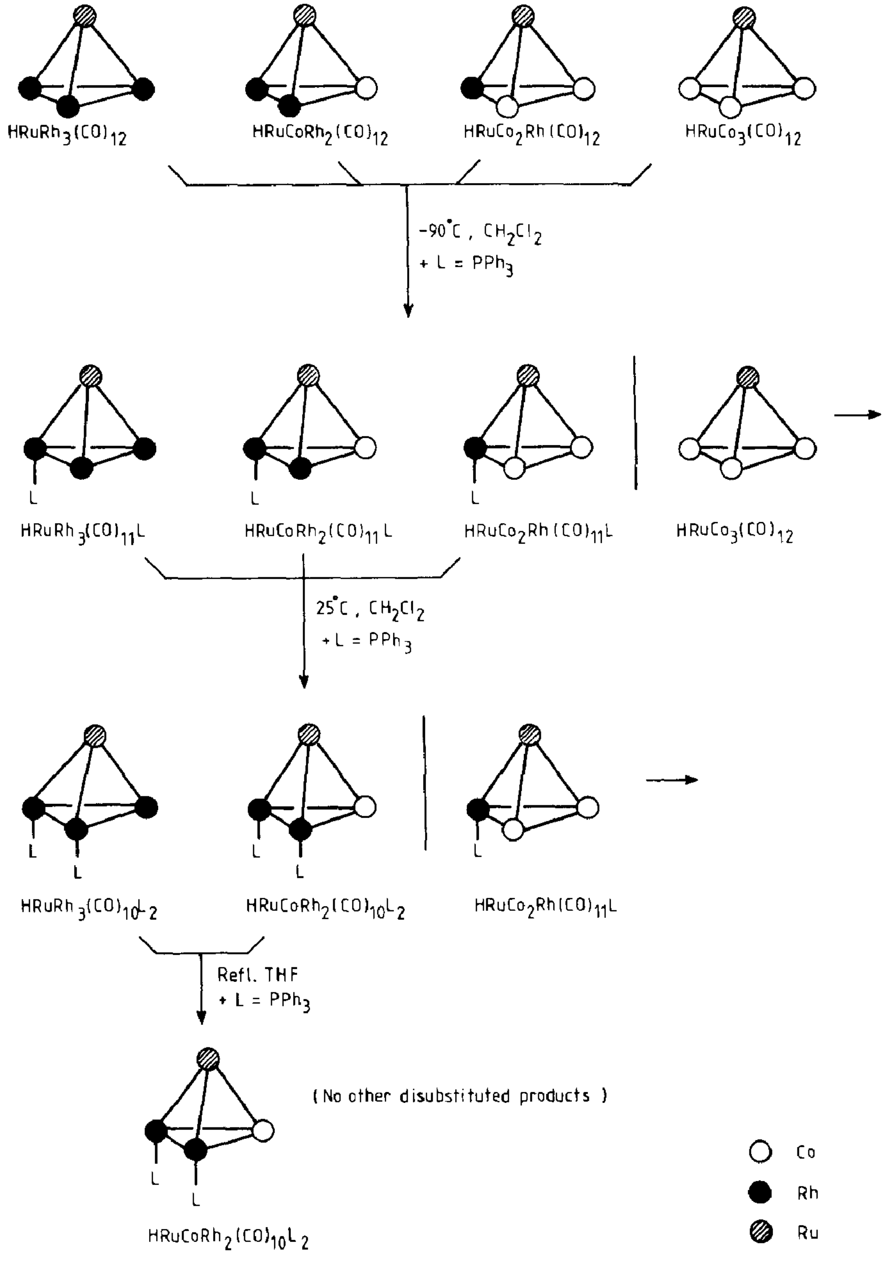

Fig. 3. A separation scheme for $HRuCo_xRh_{3-x}(CO)_{12}$ ($x = 0$–3) clusters [23].

limited structural information allows inspection of trends at a qualitative level. Figs. 5–7 show metal–metal bond length distributions for closed tetranuclear clusters. The data includes also ligand substituted derivatives. The atomic radii difference between the first and second transition series is the most prominent feature of Figs. 5 and 6 where the Fe–Fe, Fe–Ru, Ru–Ru and Co–Co, Co–Ru, Ru–Ru distance distributions are compared. The Fe–Fe and Co–Co distances are thus considerably shorter than the corresponding Ru–Ru and Rh–Rh distances. The mixed metal distances fall cleanly between the homonuclear values. The Ru–Ru distance distri-

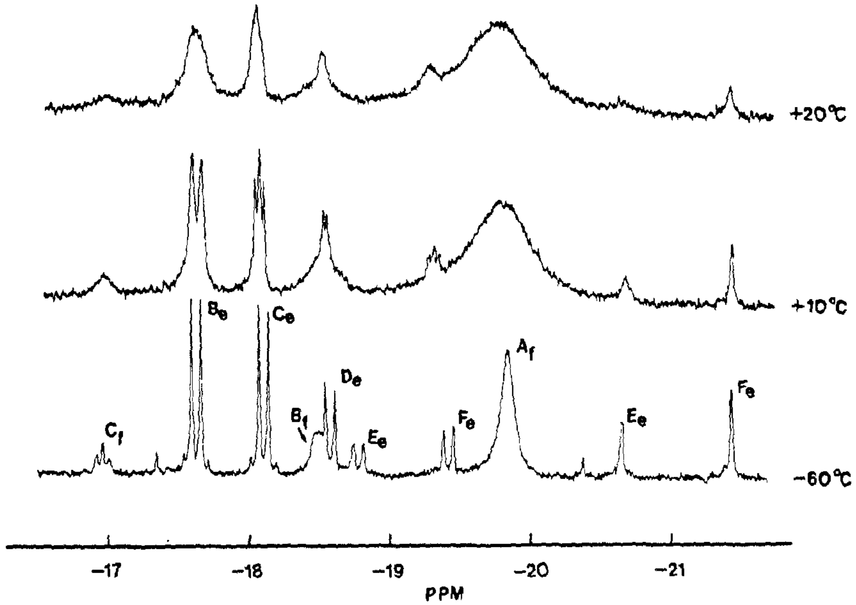

Fig. 4. Variable temperature ^1H NMR spectra of the mixture containing $HRuCo_3(CO)_{12}$ (**A**), $HRuCo_2Rh(CO)_{12}$ (**B**), $HRuCoRh_2(CO)_{12}$ (**C**), $HRuRh_3(CO)_{12}$ (**D**), $H_2Ru_2CoRh(CO)_{12}$ (**E**) and $H_2Ru_2Rh_2(CO)_{12}$ (**F**). Indexes e and f refer to edge-bridging and face-bridging hydride ligands. The signal $\mathbf{D}_f$ is at −15.5 ppm.

bution spans a long range from 2.74 Å to 3.06 Å with a gap around 2.85 Å. The short distances belong to non-bridged Ru–Ru bonds, while the longer ones are bridged by hydrogen. Carbonyl bridging does not seem to cause a significant change in the Co–Co, Rh–Rh or Co–Rh bond lengths.

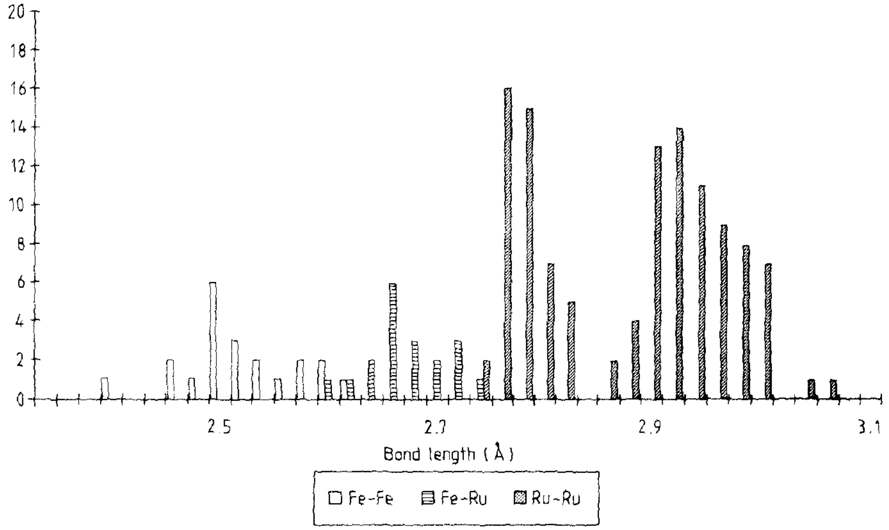

Fig. 5. Distribution of Fe–Fe, Fe–Ru and Ru–Ru distances in closed tetranuclear metal carbonyl clusters.

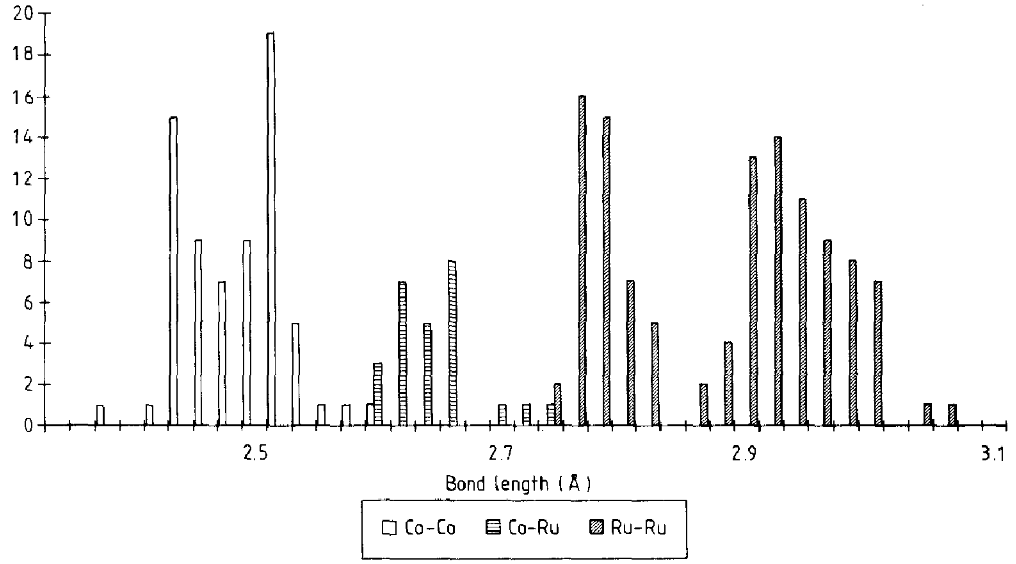

Fig. 6. Distribution of Co–Co, Co–Ru and Ru–Ru distances in closed tetranuclear metal carbonyl clusters.

The same trends are also seen in other distributions. The Rh–Rh distances appear to be shorter than the Ru–Ru distances, but it may not be a real effect, since there are no hydrogen bridged Rh–Rh distances represented in the structures (Fig. 7). The Ru–Rh distances follow closely the distribution of the Rh–Rh distances, showing also the lengthening effect due to hydrogen bridging.

This type of qualitative comparison could be useful for metal assignments in unexpected structures narrowing the probable range of a specific bond distance.

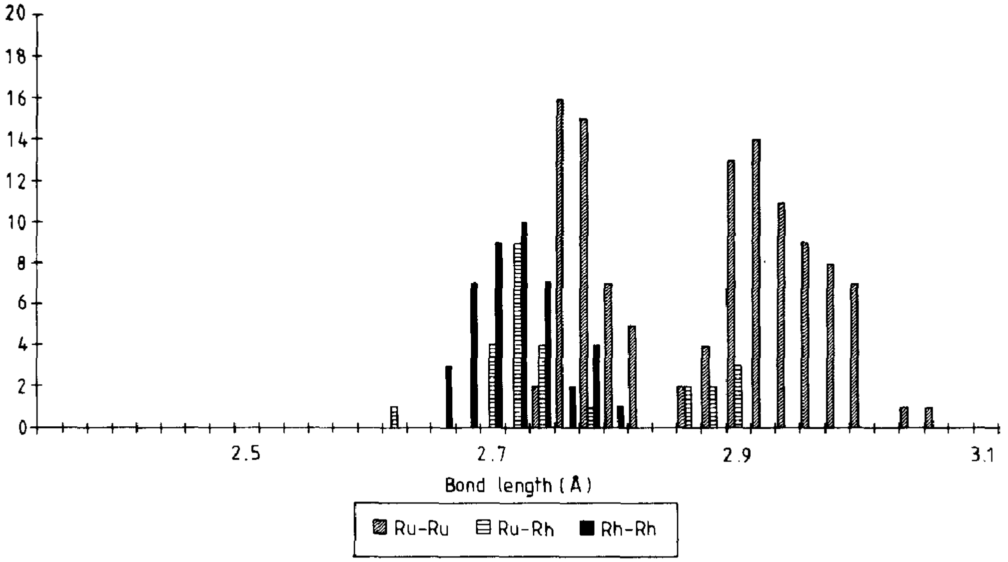

Fig. 7. Distribution of Ru–Ru, Ru–Rh and Rh–Rh distances in closed tetranuclear metal carbonyl clusters.

3.3. Structural trends

Some structural trends are immediately available. The $H_xM_4(CO)_{12}$ (M = Ru, Co or Rh) mixed metal clusters have equal numbers of ruthenium and hydrogen atoms to give them the same valence electron count. Three carbonyls bridge the metals of one of the faces of the tetrahedron when the cluster contains less than three rutheniums. Carbonyl bridged Co–Co, Rh–Rh, Co–Rh, Ru–Co and Ru–Rh bonds are represented, but not Ru(μ-CO)Ru bonds, showing the greater tendency of rhodium and cobalt to be involved with bridging carbonyls. Rutheniums prefer terminal carbonyls and hence apical sites of these clusters. In the Co–Rh mixed metal clusters apical sites are occupied by cobalt atoms (Fig. 2) [4,16]. It has been shown recently that in $M'_xM_{4-x}(CO)_{12}$ ($M' = M$ = Co, Rh or Ir; $x = 1$, 2 or 3) the tendency towards basal site occupancy is Rh $\geq$ Co $\geq$ Ir [20,21,22].

Hydrogens are either edge or face bridging. Preference for the hydrogen site can be qualitatively stated. In $H_2Ru_2Rh_2(CO)_{12}$ the Ru–Ru and Ru–Rh edges are occupied by the hydrides. This means that Ru(μ-H)Ru hydride is preferred with respect to Ru(μ-H)Rh hydrides, since the other Ru–Rh edge is not occupied. Hydrides bridge the Ru–Ru and Ru–Rh edges also in $H_2Ru_2CoRh(CO)_{12}$. However in $H_2Ru_2Co_2(CO)_{12}$, where no Ru–Rh edge is available the basal $RuCo_2$ face is occupied in addition to the Ru–Ru edge. These preferences were observed also for the $HRuCo_xRh_{3-x}(CO)_{12}$ ($x = 0$–2) parent clusters, which according to ^1H NMR spectra occur in solution as two isomers with the hydride bridging either a Ru–Rh edge or the basal trimetallic face. The Ru–Rh edge hydride is dominant (70–75%) in all the parent clusters. When no Ru–Rh edges are available as in $HRuCo_3(CO)_{12}$, the hydride bridges the Co_3 face. There is obviously not great energetic difference between these two sites since both forms coexist and also because the preference between the sites can be affected by phosphine groups. Ru(μ-H)Co bonds have been found only in $H_3Ru_3Co(CO)_{12}$ and $H_3Ru_3Co(CO)_{10}$(dppe) [7,18]. No examples of Co(μ-H)Co or Rh(μ-H)Rh hydrides have been found. One reason for such preferences could be the formal electron deficiency of ruthenium without hydride ligands. On the other hand the steric pressure caused by the hydride is obviously different in different sites.

Table 1 shows the relative amounts of the face-bridged form for the $HRuCo_xRh_{3-x}(CO)_{12}$ ($x = 0$–2) parent clusters and some of their phosphine derivatives. In the parent clusters the edge-bridging form is dominant, but in the PPh_3 derivatives this preference is inverted. The relative occupancies of the face-bridged forms decrease with different ligands in the order $PPh_3 \geq PMePh_2 \geq PMe_2Ph \geq PMe_3$. Also the relative amount of the face-bridged form decreases with the metal

Table 1

Relative amount of the $M_3(\mu$-H) face-bridged form (%) of $HRuM_3(CO)_{12-x}(PR_3)_x$ [23]

RuM_3	$RuCo_2Rh$	$RuCoRh_2$	$RuRh_3$
$x = 0$	30	29	25
$x = 1$, PMe_3	22	14	3
$x = 1$, PMe_2Ph	49	29	8
$x = 1$, $PMePh_2$	66	49	38
$x = 1$, PPh_3	81	72	60
$x = 2$, PPh_3	78	77	72

combination independent of the phosphine ligand in the order $RuCo_2Rh \geq RuCoRh_2 \geq RuRh_3$. This effect may be related to the number of Ru–Rh edges of the cluster. Three Ru–Rh edges having mutual H-exchange is probably a more stable situation against the face-bridged form than only one Ru–Rh edge. In these clusters edge-bridging hydrides are connected with equatorial phosphines, which are coordinated to the same rhodium with the hydride and further face bridging hydrides with axial phosphines. The forms that are preferred in solution can also be crystallized [23].

3.4. Spectroscopic trends

NMR spectroscopy provides data for detailed trends, since the spectra of the mixed metal clusters can be recorded and assigned also from mixtures. The ^1H NMR spectra of $HRuCo_xRh_{3-x}(CO)_{12-n}L_n$, where L = PPh_3, PMe_2Ph; and x = 0–3 illustrates the dependency of the ^1H chemical shift on the metal composition (Fig. 8). The chemical shift of the face hydride is linearly dependent on the metal

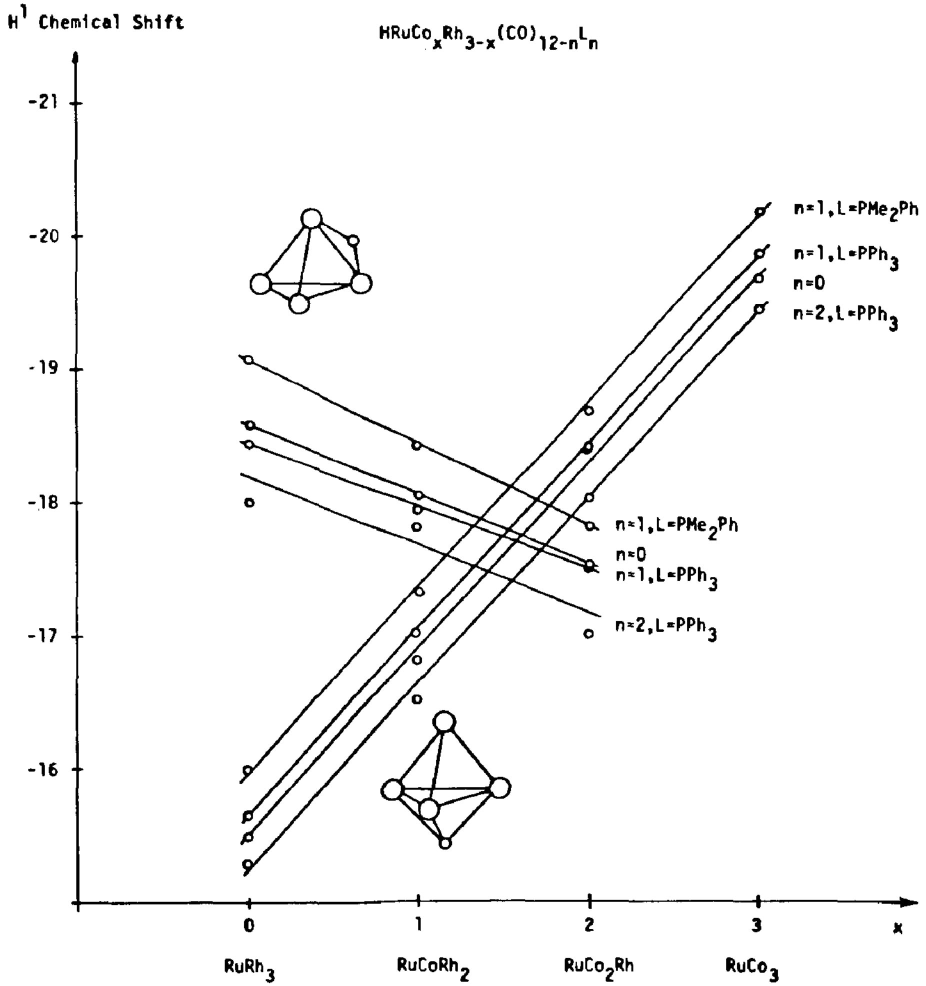

Fig. 8. 250 MHz ^1H chemical shift trends for edge- and face-bridging hydrogens in $HRuCo_xRh_{3-x}(CO)_{12-n}L_n$, where L = PPh_3, PMe_2Ph; and $x = 0$–3 and $n = 1$–2 clusters.

content of the face, the same trend is also found for the three different ligand substituted cluster series. Edge-bridged hydrides show a similar trend. However the slopes of the lines are smaller, since the hydrogen is not directly bound to the centers, where the metal composition is varied.

The same parent clusters form an example of ^{31}P NMR chemical shift trends [24]. $HRuCo_xRh_{3-x}(CO)_{12}$ ($x = 0$–3) clusters were converted to the face bridged $AuPPh_3$ derivatives. The ^{31}P NMR spectrum of the $Ph_3PAuRuCo_xRh_{3-x}(CO)_{12}$ mixture shows phosphorus chemical shift and ^{2}J(Rh–P) coupling pattern dependency on the composition of the cluster face (singlet at 53.3 ppm with $x = 3$, doublet at 56.6 ppm with $x = 2$, triplet at 59.2 ppm with $x = 1$ and quartet at 62.3 ppm with $x = 0$). Some evidence of line broadening due to cobalt is also seen in the spectra.

The chemical shift trends are often unambiguous enough to be used for characterization purposes for new cluster mixtures, and demonstrate the utility of the systematic approach.

4. Conclusions

Chemical reactivity trends of the mixed metal clusters are important for applications. The present examples illustrate only phosphine substitution preferences. The Ru–Co–Rh mixed metal clusters substitute carbonyls most easily at rhodium centers, secondly at cobalt centers. Reactivity towards other ligands is likely to produce different trends, which could be used for separation purposes. When the reactions of hydrogen, carbon monoxide and organic molecules with these clusters is studied, the role of the metal composition on their reactivity will be better understood.

Acknowledgements

Prof. Markku Ahlgren, Mr. Eero Iiskola, Mrs. Leila Alvila and Ms. Sirpa Rossi are acknowledged for fruitful collaboration and the Academy of Finland, Neste Ltd Foundation and Neste Ltd for financial support.

References

1 W.L. Wilson, R.W. Rudolph, L.L. Lohr, R.G. Taylor and P. Pyykkö, Inorg. Chem., 25 (1986) 1535.
2 R.A. Laitinen and T.A. Pakkanen, Inorg. Chem., 26 (1987) 2598.
3 E. Sappa, A. Tiripicchio, A.J. Carty and G.E. Toogood, Progress in Inorg. Chem., 35 (1987) 437.
4 S. Martinengo, P. Chini, V.G. Albano, F. Cariati and T. Salvatori, J. Organomet. Chem., 259 (1973) 379.
5 W.E. Lindsell, N.M. Walker and A.S.F. Boyd, J. Chem. Soc. Dalton Trans., (1988) 675; W.E. Lindsell, C.B. Knobler and H.D. Kaesz, J. Organomet. Chem., 296 (1985) 209.
6 R.D. Wilson, S.M. Wu, R.A. Love and R. Bau, Inorg. Chem., 17 (1978) 1271.
7 W.L. Gladfelter, G.L. Geoffroy and J.C. Calabrese, Inorg. Chem., 19 (1980) 2569.
8 E. Roland and H. Vahrenkamp, Organometallics, 2 (1983) 183.
9 J. Pursiainen, T.A. Pakkanen, B.T. Heaton, C. Seregni and R.J. Goodfellow, J. Chem. Soc. Dalton Trans., (1986) 681.
10 J. Pursiainen, T.A. Pakkanen and J. Jääskeläinen, J. Organomet. Chem., 290 (1985) 85.
11 C.H. Wei, Inorg. Chem., 8 (1969) 2394.
12 F.H. Carre, F.A. Cotton and B.A. Frenz, Inorg. Chem., 15 (1976) 380.
13 J. Pursiainen and T.A. Pakkanen, J. Organomet. Chem., 362 (1989) 375.

14 D.B.W. Yawney and F.G.A. Stone, J. Chem. Soc. A, (1969) 502; M. Hidai, M. Orisaku, M. Ue, Y. Koyasu, T. Kodama and Y. Uchida, Organometallics, 2 (1983) 292.
15 B.F.G. Johnson, J. Lewis and T.W. Matheson, J. Chem. Soc. Chem. Commun., (1974) 441.
16 M. Bojczuk, B.T. Heaton, S. Johnson, C.A. Ghilardi and A. Orlandini, J. Organomet. Chem., 341 (1988) 473.
17 J. Pursiainen and T.A. Pakkanen, J. Organomet. Chem., 315 (1986) 353.
18 J. Pursiainen and T.A. Pakkanen, J. Organomet. Chem., 309 (1986) 187.
19 H. Bantel, W. Bernhardt, A.K. Powell and H. Vahrenkamp, Chem. Ber., 121 (1988) 1247.
20 V.G. Albano, G. Ciani and S. Martinengo, J. Organomet. Chem., 78 (1974) 265.
21 S. Martinengo, P. Chini, F. Cariati and T. Salvatori, J. Organomet. Chem., 59 (1973) 379.
22 J. Evans, B.F.G. Johnson, J. Lewis, T.W. Matheson and J.R. Norton., J. Chem. Soc. Dalton Trans., (1978) 626.
23 J. Pursiainen, M. Ahlgren and T.A. Pakkanen, unpublished results.
24 J. Pursiainen, M. Ahlgren and T.A. Pakkanen, J. Organomet. Chem. 297 (1985) 391.